Journal of Engineering Physics and Thermophysics, Vol. 73, No. 2, 2000

HYDRODYNAMICS AND HEAT TRANSFER IN COOLING SYSTEMS WITH INTERSECTING CHANNELS. 3. EFFECT OF THE ANGLE OF FLOW AND THE NUMBER OF STAGES

Yu. I. Shanin, O. I. Shanin, and V. A. Afanas'ev

UDC 536.35:62-405.8; 621.375

Results of further investigation of some variants of wafer structures are given. The effect of the angle of flow on the hydraulic resistance and heat transfer at Re numbers of $1 \cdot 10^2$–$2 \cdot 10^4$ is revealed. The temperature field of a two-stage system is analyzed. It is shown that a size reduction of the structure and an increase in the number of stages make it possible to obtain the maximum possible coefficient of reduced heat transfer $(2.5–2.8) \cdot 10^5$ W/(m^2·K).

The main objective of the use of cooling systems with intersecting channels is intensification of heat transfer. In the literature [1] results of an investigation of the hydraulic characteristics of such structures in the air-to-air heat exchanger for cooling radioelectronic components of the 3M company installed aboard the American Space Shuttle are given. The experimentally investigated structure represented essentially a two-dimensional tube bank of staggered diamond-shaped rods replacing tubes. The use of such structures was proposed earlier for cooling laser mirrors [2] and was considered in greater detail in [3] for structures of substantial relative height ($h_{ch}/\delta_{ch} \approx 7$–$9$) that are similar to a two-dimensional bank.

Earlier we studied experimentally the hydraulic resistance and heat transfer in cooling systems with intersecting channels with low heights ($h_{ch}/\delta_{ch} \approx 1$–$3$) both for individual models [4] and for groups of models selected in a special manner [5, 6] to obtain and generalize data.

Given below are results of an experimental investigation of the hydraulic resistance, heat transfer, and temperature field for a wafer structure with an intersection angle of the channels $\varphi = 60^\circ$ as functions of the angle of flow about it (or, put another way, the angle of attack γ). Dependences of the relative hydraulic resistance and the heat transfer on the angle of attack have been obtained for structures with $\varphi = 60$ and 90°. The thermal state of two two-stage wafer cooling systems has also been investigated.

The cooling systems (so-called wafer structures) were produced by milling, in the material, channels of the same height h_{ch} (Fig. 1) mutually intersecting at an angle (in our case, $\varphi = 60^\circ$). The thermohydraulic characteristics were studied on special copper models ($\lambda = 380 \pm 10$ W/(m·K)) consisting of two plates soldered together. A cooling system is formed in one of them. The plates' lateral surfaces are covered with lids. The length, width, and height of the model were 110, 30, and 12 mm, respectively. The geometry of the models and their characteristics are given in Table 1 with straight-through numbering of the models that continues the one begun in [5] being kept. Each of the models is drained by four holes 1 mm in diameter for tapping the static pressure; the holes are located at a distance $l = 70$–80 mm and are equidistant from the inlet and outlet of the model. The model was glued into flanges and was fixed to the supply and discharge collectors. The conditions at the inlet to the model corresponded to the conditions of outflow from a large volume and provided a uniform velocity profile at the inlet. A more detailed description of the methodological procedure of the thermohydraulic experiment is given in [5, 6]. Here we will just mention that the hydraulic resistance was

State Research Institute of the Scientific-Production Association "Luch," Podol'sk, Russia. Translated from Inzhenerno-Fizicheskii Zhurnal, Vol. 73, No. 2, pp. 214-223, March–April, 2000. Original article submitted December 11, 1998.

1062-0125/00/7302-0209$25.00

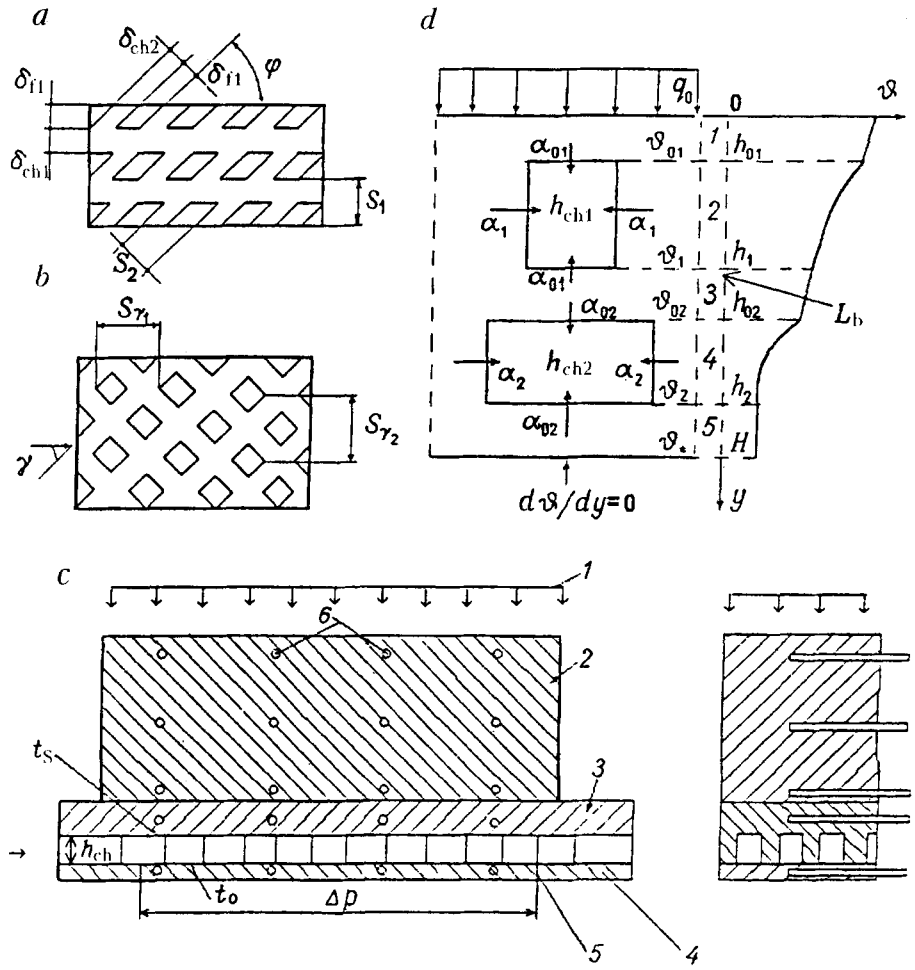

Fig. 1. View of structures and the experimental scheme: a) straight-line scheme (plan); b) staggered scheme (plan); c) scheme of an experimental portion [1) ohmic heater; 2) thermal wedge; 3) monolithic plate with a cooling system; 4) connected plate; 5) pressure tap; 6) thermocouples]; d) scheme of a two-stage system [1) upper plate; 2 and 4) wafer structure; 3) intermediate plate; 5) lower plate.

TABLE 1. Characteristics of the Investigated Models of Cooling Systems

No. of model	γ, deg	δ_{ch} and h_{ch}, mm	d_h, mm	δ_f, mm	ε	P, m^2/m^3
18	0	1.07; 3.06	1.59	1.44	0.672	1350
19	15(45)	1.08; 3.08	1.60	1.49	0.663	1335
20	30(60)	1.05; 3.05	1.56	1.50	0.654	1352
21	75	1.03; 3.13	1.55	1.49	0.650	1355
22	90	1.02; 3.04	1.53	1.47	0.653	1375
23	105	1.02; 3.09	1.54	1.47	0.652	1369
24	120	0.92; 3.06	1.42	1.59	0.600	1398

measured by the known pressure gradient Δp on the model's length l and the flow rate G of the liquid, for which water at room temperature (t_{liq} = 15–25°C) was used. The heat-transfer experiments were conducted by a thermal-wedge method that provided a uniform heat flux in four measuring cross sections along the model (Fig. 1c).

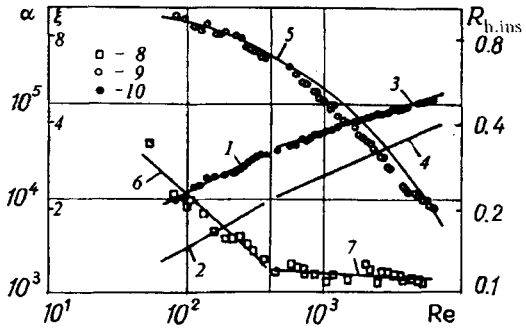

Fig. 2. Thermohydraulic characteristics of model 20 vs. Reynolds number: 1) $\alpha_{red} = 383\ Re_2^{0.745}$, W/(m^2·K) ($67 < Re_2 < 400$); 2) $\alpha_0 = 66.4\ Re_2^{0.835}$, W/(m^2·K); 3) $\alpha_{red} = 2200\ Re_2^{0.46}$, W/(m^2·K) ($4\cdot10^2 < Re_2 < 7.4\cdot10^3$); 4) $\alpha_0 = 235\ Re_2^{0.63}$, W/(m^2·K); 5) $R_{h.ins.calc}$, calculated "heat-insulation" coefficient; 6) $\xi_2 = 17\ Re_2^{-0.44}$ ($48 < Re_2 < 400$); 7) $\xi_2 = 1.4\ Re_2^{-0.0255}$($4\cdot10^2 < Re_2 < 7\cdot10^3$); 8-10) experiment; 8) ξ_2; 9) α_{red}; 10) $R_{h.ins.exp}$, experimental "heat-insulation" coefficient.

The hydraulic diameter of the channel d_h was taken as the characteristic dimension when the results were generalized. The filtration rate w_{filtr}, the average rate $w_2 = w_{filtr}\varepsilon^{-1}$, and the maximum rate $w_1 = w_{filtr}\varepsilon_m^{-1}$ were used as the characteristic rate, where ε_m is determined from the equation $\varepsilon_m^2 - 2\varepsilon_m + \varepsilon = 0$. The use of different rates is appropriate for comparison with data from literature sources: the rate w_{filtr} is preferable when the wafer structure is considered as a porous body, w_1 – for comparison with a channel cooling system, w_2 – for flow about the same structure at different angles of attack γ. These rates were used to obtain the corresponding Reynolds numbers $Re_i = w_i d_h/\mu_{liq}$ (with a maximum error of 5–6%) and coefficients of hydraulic resistance $\xi_i = \Delta p/[\rho w_i^2/2(d_h/l)]$ (with a maximum error of 10–15%) (hereinafter indirect values of measurements are determined with a confidence probability of 0.95).

The temperature field of the thermal wedge and the model was measured and the results were used to calculate the following quantities: the heat flux q_0 with a maximum error of 3–5%, the reduced heat-transfer coefficient α_{red} with an error of 10–16% ($\alpha_{red} = q_0/(t_s - t_{liq})$, t_{liq} is the mass-mean temperature of the liquid in the measurement cross section, t_s is the temperature of the cooled surface of the model), the conventional "heat-insulation" coefficient $R_{h.ins}$ of the lower plate of the model with an error of 5–20% ($R_{h.ins} = (t_{base} - t_{liq})/(t_s - t_{liq})$, t_{base} is the temperature of the lower, heat-insulated plate), exhibiting the ratio of the excess temperatures of the heat-insulated and thermally loaded plates and indicating the ratio of the heat flux q_1 that would pass into the main structure (in the absence of a boundary condition of heat insulation) to the total heat flux q_0 (since $R_{h.ins} = \alpha_{red}(t_{base} - t_{liq})/[\alpha_{red}(t_s - t_{liq})] = q_1/q_0$).

The quantities α_{red} and $R_{h.ins}$ characterize the temperature field of the model. At the same time, α_{red} describes the effective heat transfer [5, 6] and, along with the surface heat transfer of the model's unfinned part (the averaged heat-transfer coefficient on this surface α_0), takes into account the contribution of the heat transfer of the prismatic fins (the averaged coefficient of heat transfer from the fins α) and the lower plate.

In calculating the thermally deformed state of a laser mirror (or another thermal-protection device) equipped with these cooling systems, the coefficients α_{red} and $P_{h.ins}$ unambiguously describe a one-dimensional temperature field along the height of the cooling-system material [6].

The investigated group of models had the same intersection angle of the channels $\varphi = 60°$, and they differed only in the angle of attack $\gamma = 0$–$120°$. By analogy with tube banks, with variation in the angle of attack γ, there can be two cases of axisymmetric flow about a wafer structure: with a straight-line arrangement of the fins ($\varphi = 60°$, $\gamma = 0$, $60°$) and with a staggered one ($\varphi = 60°$, $\gamma = 30$, $120°$). The obtained thermohydraulic characteristics of the models (the coefficient of hydraulic resistance $\xi_2 = (2\Delta p d_h)/(\rho w_2^2 l)$, the coefficient of reduced heat transfer α_{red}, and the heat-insulation coefficient $R_{h.ins}$) were plotted against the number Re_2; the characteristic form of the dependences is given in Fig. 2 for model 20. The experiments were conducted in a

TABLE 2. Generalization of Experimental Results on Hydraulic Resistance and Heat Transfer in the Turbulent Region of Re Numbers

No. of model	Resistance		Heat transfer α_{red}, W/(m^2·K)		$\alpha(Re_2)$, W/(m^2·K)	$K_1(Re_1)$	$K_v(Re_2)$	$K_\xi(\xi Re_2^3)$
	Re range	A_0, n_0	Re range	A_1; n_1	A_2; n_2	A_3; n_3	A	A_4; n_4
18	$(3–80)\cdot10^2$	0.75; –0.0355	$(3.2–80)\cdot10^2$	975; 0.55	89.2; 0.74	0.090; 0.74	81	0.13; 0.25
19	$(5.5–84)\cdot10^2$	1.70; –0.0834	$(3.0–80)\cdot10^2$	1260; 0.52	124; 0.70	0.125; 0.70	113	0.15; 0.24
20	$(4–70)\cdot10^2$	1.40; –0.0254	$(4–74)\cdot10^2$	2200; 0.46	235; 0.63	0.240; 0.63	220	0.30; 0.21
21	$(1.7–56)\cdot10^2$	2.90; –0.0212	$(2–50)\cdot10^2$	700; 0.51	172; 0.70	0.168; 0.70	160	0.18; 0.23
22	$(3.6–25)\cdot10^2$	8.20; –0.0292	$(3–30)\cdot10^2$	1700; 0.54	157; 0.74	0.148; 0.74	140	0.12; 0.22
23	$(1.3–25)\cdot10^2$	13.40; –0.0447	$(2.8–20)\cdot10^2$	2770; 0.48	307; 0.66	0.300; 0.66	290	0.23; 0.22
24	$(2.3–20)\cdot10^2$	11.70; –0.01	$(3–20)\cdot10^2$	1750; 0.56	150; 0.78	0.127; 0.78	130	0.10; 0.26

wide range of Reynolds numbers Re = 40–$8\cdot10^3$, with the lower Reynolds number determined by the minimum possible flow rate through the model 1 g/sec and the upper number governed by the maximum possible pressure difference on the working portion ΔP = 0.65 MPa. The same figure gives dependences for the surface coefficients of heat transfer α_s identified based on the assumption of approximate equality of the coefficients of surface heat transfer on the fin α and on the unfinned portion of the heat exchanger α_0 (the identification procedure is realized by the methods presented in [6]). By analogy with [6] the results in the indicated ranges of Re_2 number are generalized in different coordinates and are summarized in Table 2, where $K_1 = Nu\ Pr^{-1/3} = f_1(Re_1)$, $K_v = Nu_v\ Pr^{-1/3} = f_2(Re_2)$, and $K_\xi = Nu_2\ Pr^{-1/3} = f_3(\xi_2 Re_2^3)$ (as has already been mentioned, ξ_2 and Nu are obtained in a wide Re_2 range and differ by a change in the character of the behavior with increase in the number Re_2, but here consideration is given only to the regions of turbulent flow). The coefficients A_0, A_1, A_2, A_3, A_4, and A and the exponents n_0, n_1, n_2, n_3, and n_4 ($n_2 = n_3$) in Table 2 were obtained by approximation of experimental data using the least-squares method and are given, for compactness, without the additions $\pm\Delta A_i$ and $\pm\Delta n_i$ that allow for the variance of the deviations. Use of the coordinates K_1–Re enables us to compare wafer cooling systems with channel ones [7, 8]. The coordinates K_v – Re present results for the volumetric heat-transfer coefficient α_v ($Nu_v = \alpha_v d_h/\lambda_{liq}$). To reveal the energy efficiency of the investigated and other systems and to find the interrelationship between hydraulic resistance and heat transfer in structures with a complex topology based on the local-similarity method and Kolmogorov's velocity scale by analogy with [9], we presented results in the coordinates $K_\xi = Nu_2\ Pr^{-1/3} = f_3(\xi_2 Re_2^3)$ – Re_2.

We selected the variant with a straight-line wafer structure as the base variant for revealing the dependence of the resistance $\xi_2(\gamma)$ and the heat transfer $Nu(\gamma)$ on the angle of attack. By generalization of the results using the least-squares method we obtained the following power-law dependences for the straight-line wafer system:

$$\xi_2 = 0.75\ Re_2^{-0.036}, \quad K_1 = Nu\ Pr^{-1/3} = 0.75\ Re_1^{0.74} \tag{1}$$

for $\varphi = 60°$, $\gamma = 0$, $60°$, and $3\cdot10^2 < Re_2 < 8\cdot10^3$;

$$\xi_2 = 0.72\ Re_2^{-.012}, \quad K_1 = Nu\ Pr^{-1/3} = 0.115\ Re_1^{0.73} \tag{2}$$

for $\varphi = 90°$, $\gamma = 0°$, and $8\cdot10^2 < Re_2 < 1.5\cdot10^3$.

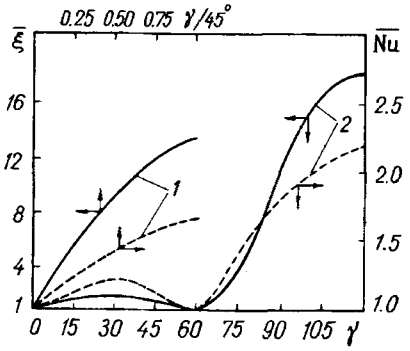

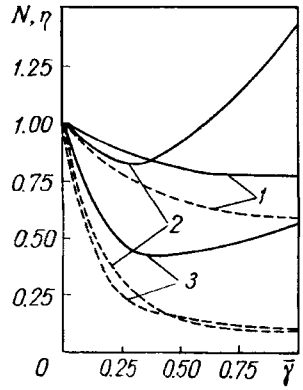

Fig. 3. Relative resistance $\bar{\xi}$ and heat transfer $\overline{Nu}$ vs. angle of flow: 1) $\varphi = 90^\circ$ and $Re_2 = 2.5 \cdot 10^{-3}$; 2) $\varphi = 60^\circ$. γ, deg.

Fig. 4. Quantities N and η vs. angle of flow $\bar{\gamma}$: 1) $\varphi = 60^\circ$, $0^\circ \le \gamma \le 30^\circ$, $\gamma = \gamma/30$, $Re_2 = 2 \cdot 10^3$; 2) $\varphi = 60^\circ$, $60^\circ \le \gamma \le 120^\circ$, $\gamma = (\gamma - 60)/60$, $Re_2 = 2 \cdot 10^3$; 3) $\varphi = 90^\circ$, $0^\circ \le \gamma \le 45^\circ$, $\gamma = \gamma/45$, $Re_2 = 2.5 \cdot 10^3$; the solid curves show N and the dashed curves show η.

Figure 3 presents plots of the relative resistance $\bar{\xi} = \xi_2(\gamma)/\xi_2(\gamma = 0^\circ)$ and the relative heat transfer $\overline{Nu} = Nu(\gamma)/Nu(\gamma = 0^\circ)$ against the angle of attack γ obtained by normalization to the characteristictics for the base variant (formulas (1) and (2)) at a constant Reynolds number. The feature common to all the structures is an increase in resistance and heat transfer with γ. Here, passage from the straight-line structure to the staggered one is characterized by an increase in hydraulic resistance (by a factor of 14–16) that predominates over heat transfer (by a factor of 1.6–2.2).

For approximating experimental data on the hydraulic resistance and the heat transfer as functions of the angle by a polynomial (of n-th order), we obtained the following formulas:

$$\bar{\xi} = -4.267\bar{\gamma}^4 + 6.4\bar{\gamma}^3 - 9.333\bar{\gamma}^2 + 19.6\bar{\gamma} + 1, \tag{3}$$

$$\overline{Nu} = -0.853\bar{\gamma}^4 + 1.493\bar{\gamma}^3 - 1.067\bar{\gamma}^2 + 1.067\bar{\gamma} + 1 \tag{4}$$

at $\varphi = 90^\circ$, $\bar{\gamma} = \gamma/45$, and $0^\circ < \gamma < 45^\circ$;

$$\bar{\xi} = 0.213\bar{\gamma}^4 - 0.427\bar{\gamma}^3 - 4.013\bar{\gamma}^2 + 4.227\bar{\gamma} + 1, \tag{5}$$

$$\overline{Nu} = 2.944\bar{\gamma}^4 - 5.888\bar{\gamma}^3 + 2.856\bar{\gamma}^2 + 0.088\bar{\gamma} + 1 \tag{6}$$

at $\varphi = 60^\circ$, $\bar{\gamma} = \gamma/30$, and $0^{\circ <} \gamma < 30^\circ$;

$$\bar{\xi} = 29.867\bar{\gamma}^4 - 102.4\bar{\gamma}^3 + 95.733\bar{\gamma}^2 - 6\bar{\gamma} + 1, \tag{7}$$

$$\overline{Nu} = 3.413\bar{\gamma}^4 - 7.467\bar{\gamma}^3 + 4.427\bar{\gamma}^2 + 0.827\bar{\gamma} + 1 \tag{8}$$

at $\varphi = 60^\circ$, $\bar{\gamma} = (\gamma - 60)/60$, and $60^\circ < \gamma < 120^\circ$.

The ratio $\eta = \overline{Nu}/\bar{\xi}$ (Fig. 4) shows by what factor the heat transfer exceeds the resistance as γ increases. With a prescribed heat power of the thermal-protection device and the heat-exchange surface the intensification of heat transfer is characterized by the expenditure of power on pumping the heat-transfer agent. Having the characteristics for the base variant in the form of the power functions $Nu = C_1 Re^n$ and $\xi_2 =$

$C_2\mathrm{Re}^m$ (where C_1 and C_2 are constants) and the dependences $\bar{\xi}(\bar{\gamma})$ and $\overline{\mathrm{Nu}}(\bar{\gamma})$, by analogy with [10] the ratio of the powers expended on pumping the heat-transfer agent is characterized by the combination

$$N = \mathrm{Nu}^{(m+3)/n}/\xi, \tag{9}$$

where $(m+3)/n = 4$ (for $\varphi = 60^\circ$) and 3.93 (for $\varphi = 90^\circ$).

This combination compares the heat power of devices with identical flow rates of the heat-transfer agent and hydraulic resistances and is presented in Fig. 4 as a function of the angle γ. Its behavior differs from the behavior of $\eta = \overline{\mathrm{Nu}}/\bar{\xi}$ by the fact that, for some cases, there is a minimum point in N with its subsequent increase. The quantity N itself differs from 1 not as strongly as η. For $\varphi = 60^\circ$, $N \geq 1$ at $\gamma > 96^\circ$.

Let us consider some measures [6] aimed at increasing further the heat transfer in wafer structures, among them the use of multistage systems and size reduction of the structure. We take, as an example, a two-stage cooling system that is a combination of straight-line (on the upper stage) and staggered (on the lower stage) schemes of arrangement of the fins. This arrangement ensures a decrease in the flow rate of the heat-transfer agent while retaining a high efficiency of the heat transfer as compared to the case of a straight-line scheme for the two stages.

The thermal state of multistage flow cooling systems is analyzed in [8] in detail. Here we give the solution for the temperature field of a two-stage cooling system without a derivation. The scheme of the problem solved is presented in Fig. 1d, while the basic assumptions and the complete mathematical formulation of the problem are contained in [6-8]. The temperature field over the thickness of a cooling system manufactured from a homogeneous material is determined in general form by the formulas

$$\vartheta_{01} = q_0 \left[1/\alpha_{\mathrm{red}1} + (h_{01} - y)/\lambda\right] \tag{10}$$

for the upper plate,

$$\vartheta_1 = \frac{q_0}{\alpha_{\mathrm{red}1}} \frac{\cosh\left[m_1 (h_1 - y) + \varphi_1\right]}{\cosh\left[m_1 (h_1 - h_{01}) + \varphi_1\right]} \tag{11}$$

for the fins of the first stage,

$$\vartheta_{02} = q_0 \left[\frac{1}{\alpha_{\mathrm{red}2}} + \frac{h_{02} - y}{\lambda}\right] \frac{\sinh(\varphi - \varphi_{01})}{\sinh\left[m_1 (h_1 - h_{01}) + \varphi_{01} + \varphi_1\right]} \tag{12}$$

for the intermediate plate between the fins,

$$\vartheta_2 = \frac{q_0}{\alpha_{\mathrm{red}2}} \frac{\cosh\left[m_2 (h_2 - y) + \varphi_{02}\right]}{\cosh\left[m_2 (h_2 - h_{02}) + \varphi_{02}\right]} \frac{\sinh(\varphi_1 - \varphi_{01})}{\sinh\left[m_1 (h_1 - h_{01}) + \varphi_{01} + \varphi_1\right]} \tag{13}$$

for the fins of the second stage,

$$\vartheta_* = \frac{q_0}{\alpha_{\mathrm{red}2}} \frac{\cosh \varphi_{02}}{\cosh\left[m_2 (h_2 - h_{02}) + \varphi_{02}\right]} \frac{\sinh(\varphi_1 - \varphi_{01})}{\sinh\left[m_1 (h_1 - h_{01}) + \varphi_{01} + \varphi_1\right]} \tag{14}$$

for the lower plate.

The reduced coefficients of heat transfer are determined under the condition of different coefficients of surface heat transfer on the plate walls and the fins (in the general form, $\alpha_{01} \neq \alpha_1$ and $\alpha_{02} \neq \alpha_2$) by the formulas

$$\alpha_{\mathrm{red}1} = \varepsilon_1 \alpha_{01} + (1 - \varepsilon_1) \lambda m_1 \tanh\left[m_1 (h_1 - h_{01}) + \varphi_1\right] =$$

$$= \frac{(1-\varepsilon_1)\,\lambda m_1}{\cosh \varphi_{01}} \frac{\sinh\left[m_1 (h_1 - h_{01}) + \varphi_{01} + \varphi_1\right]}{\cosh\left[m_1 (h_1 - h_{01}) + \varphi_1\right]} \tag{15}$$

for reduction to the upper plate (i.e., with allowance for all the stages of the system),

$$\alpha_{red2} = \varepsilon_2\,\alpha_{02} + (1-\varepsilon_2)\,\lambda m_2 \tanh\left[m_2 (h_2 - h_{02}) + \varphi_{02}\right] =$$

$$= \frac{(1-\varepsilon_2)\,\lambda m_2}{\cosh \varphi_{02}} \frac{\sinh\left[m_2 (h_2 - h_{02}) + 2\varphi_{02}\right]}{\cosh\left[m_2 (h_2 - h_{02}) + \varphi_{02}\right]} \tag{16}$$

for reduction to the intermediate plate (i.e., with allowance just for the lower stage), where $m_i = \sqrt{2\alpha_i/(\lambda\delta_{ti})}$, $i = 1, 2$; ε_i is the porosity of the i-th stage;

$$\tanh \varphi_{0i} = \frac{\varepsilon_i}{1-\varepsilon_i} \frac{\alpha_{0i}}{\lambda m_i} \le 1 \quad (i = 1, 2)\,;$$

$$\tanh \varphi_i = \frac{\varepsilon_1}{1-\varepsilon_1} \frac{\alpha_{01}}{\lambda m_1} + \frac{1}{(1-\varepsilon_1)\,\lambda m_1} \frac{1}{\dfrac{h_{02} - h_1}{\lambda} + \dfrac{1}{\alpha_{red2}}} \le 1\,.$$

Under the assumption $\alpha_{01} \approx \alpha_1$ and $\alpha_{02} \approx \alpha_2$ (this proposition is substantiated in [6]) for the channel heights h_{ch1} and h_{ch2} and the thickness of the intermediate plate (baffle) L_b formulas (15) and (16) will be simplified:

$$\alpha_{red1} = \varepsilon_1\,\alpha_1 + (1-\varepsilon_1)\,\lambda m_1 \tanh\left(m_1 h_{ch1} + \varphi_0\right), \tag{17}$$

$$\alpha_{red2} = \varepsilon_2\,\alpha_2 + (1-\varepsilon_2)\,\lambda m_2 \tanh\left(m_2 h_{ch2} + \varphi_2\right), \tag{18}$$

where

$$\tanh \varphi_1 = \frac{\varepsilon_1}{1-\varepsilon_1} \frac{\alpha_1}{\lambda m_1}; \quad \tanh \varphi_2 = \frac{\varepsilon_2}{1-\varepsilon_2} \frac{\alpha_2}{\lambda m_2};$$

$$\tanh \varphi_0 = \frac{\varepsilon_1}{1-\varepsilon_1} \frac{\alpha_1}{\lambda m_1} + \frac{1}{(1-\varepsilon_1)\,\lambda m_1} \frac{1}{\dfrac{L_b}{\lambda} \dfrac{1}{\alpha_{red2}}}.$$

With equality of the pressure difference along the system's length in the stages and power dependences of the coefficient of hydraulic resistance in the stages $\xi(1) = a_1 \mathrm{Re}^{n_1}$ and $\xi(2) = a_2 \mathrm{Re}^{n_2}$ the ratio of the flow rates in the first $G(1)$ and second $G(2)$ stages is proportional to the ratio of the Reynolds numbers $G(1)/G(2) \cong \mathrm{Re}(1)/\mathrm{Re}(2)$, from which

$$\mathrm{Re}\,(2) = \left(\frac{a_1}{a_2}\right)^{1/(2+n_2)} \mathrm{Re}\,(1)^{(2+n_1)/(2+n_2)}. \tag{19}$$

If there are approximation formulas for the surface coefficient of heat transfer $\alpha(1) = A_1 \mathrm{Re}(1)^{m_1}$ and $\alpha(2) = A_2 \mathrm{Re}(2)^{m_2}$, under the condition of the same pressure gradient $\Delta p/l$ over the stages there is the relationship

$$\alpha\,(2) = A_2 \left[\left(\frac{a_1}{a_2}\right)^{1/(2+n_2)} \mathrm{Re}\,(1)^{(2+n_1)/(2+n_2)}\right]^{m_2}. \tag{20}$$

TABLE 3. Thermophysical Characteristics of a Two-Stage Wafer Cooling System with $\varphi = 90°$

	$Re(1)\cdot 10^{-3}$	1.5	2.0	5.0	10.0	16
Upper stage	$\alpha_{01}\cdot 10^{-5}$, W/(m^2·K)	0.227	0.280	0.550	0.910	1.290
	$\alpha_{red1}\cdot 10^{-5}$, W/(m^2·K)	0.456	0.557	0.956	1.416	1.845
	$R_{h.ins1}$	0.665	0.614	0.434	0.300	0.220
Lower stage	$Re(2)\cdot 10^{-3}$	0.410	0.540	1.280	2.450	3.810
	$\alpha_{02}\cdot 10^{-5}$, W/(m^2·K)	0.197	0.231	0.387	0.570	0.744
	$\alpha_{red2}\cdot 10^{-5}$, W/(m^2·K)	0.410	0.470	0.720	0.980	1.210
Two stages	$\alpha_{red}(2)\cdot 10^{-5}$, W/(m^2·K)	0.570	0.652	1.050	1.452	1.867
	$R_{h.ins}(2)$	0.256	0.193	0.105	0.052	0.030
	$\alpha_{red}(2)/\alpha_{red1}$	1.250	1.170	1.100	1.030	1.010
	$R_{h.ins}(2)/R_{h.ins1}$	0.385	0.314	0.242	0.173	0.136

Let us perform evaluations for two cooling systems. First we consider a combination of systems realized in models 6 and 10 [5, 6], for which the following characteristics were obtained earlier:

$$\xi_2 = 0.721\ \mathrm{Re}_2^{-0.121} \quad \text{at} \quad 800 \le \mathrm{Re}_2 \le 1.5\cdot 10^4,$$

$$\alpha_{red} = 721.3\ \mathrm{Re}_2^{0.573},\quad \alpha = 104.7\ \mathrm{Re}_2^{0.733} \quad \text{at} \quad 2\cdot 10^4 \le \mathrm{Re}_2 \le 1.6\cdot 10^4 \tag{21}$$

for the upper stage, $\varphi = 90°$, $\gamma = 0°$, $\varepsilon_1 = 0.77$, $d_{h1} = 1.63$ mm, $\delta_{ch1} = \delta_{f1} = 1.6$ mm, and $h_{ch1} = 1.6$ mm;

$$\xi_2 = 4.01\ \mathrm{Re}_2^{-0.0019} \quad \text{at} \quad 400 \le \mathrm{Re}_2 \le 4\cdot 10^3,$$

$$\alpha_{red} = 2586.4\ \mathrm{Re}_2^{0.464},\quad \alpha = 537.3\ \mathrm{Re}_2^{0.6} \quad \text{at} \quad 400 \le \mathrm{Re}_2 \le 3\cdot 10^3 \tag{22}$$

for the lower stage, $\varphi = 90°$, $\gamma = 45°$, $\varepsilon_2 = 0.796$, $d_{h2} = 1.68$ mm, and $\delta_{ch2} = \delta_{f2} = h_{ch2} = 1.6$ mm.

For the numbers Re in the stages, we obtain based on (19) the relationship between the second and first stages

$$\mathrm{Re}\ (2) = 0.424\ \mathrm{Re}\ (1)^{0.94}. \tag{23}$$

By the formulas obtained we calculated the heat transfer for different Re numbers (Table 3). The surface coefficient of heat transfer α, the reduced coefficient of heat transfer α_{red}, and the "heat-insulation" coefficient $R_{h.ins}$ are determined as functions of the number Re in the rows of the table. Calculations in which the stages are taken separately and the relationship between them is determined from the Reynolds number by formula (23) are given first. Next, with account for these two quantities the reduced coefficient of heat transfer of the two-stage system $\alpha_{red}(2)$ and the heat-insulation coefficient $R_{h.ins}(2)$ are determined and their comparison with the upper stage is given in the form of the combinations $\alpha_{red}(2)/\alpha_{red1}$ and $R_{h.ins}(2)/R_{h.ins1}$, where α_{red1} and $R_{h.ins1}$ are only for the first stage of the cooling system.

The next two-stage scheme is "realized" as a combination of staggered systems – models 14 and 10 [5, 6] with an intersection angle of the channels of the upper stage $\varphi = 60°$, and for it we obtained the following characteristics:

$$\xi_2 = 3.14\ \mathrm{Re}_2^{-0.115} \quad \text{at} \quad 140 \le \mathrm{Re}_2 \le 4\cdot 10^3,$$

TABLE 4. Thermophysical Characteristics of a Two-Stage Wafer Cooling System with $\varphi = 60^\circ$

	$Re(1)\cdot10^{-3}$	0.6	0.8	1.0	2.0	4.0	6.0
Upper stage	$\alpha_{01}\cdot10^{-5}$, W/(m^2·K)	0.234	0.290	0.332	0.520	0.813	1.060
	$\alpha_{red1}\cdot10^{-5}$, W/(m^2·K)	0.487	0.570	0.640	0.916	1.300	1.590
	$R_{h.ins1}$	0.654	0.608	0.571	0.450	0.328	0.263
Lower stage	$Re(2)\cdot10^{-3}$	0.370	0.485	0.600	1.150	2.210	3.240
	$\alpha_{02}\cdot10^{-5}$, W/(m^2·K)	0.200	0.232	0.263	0.390	0.580	0.724
	$\alpha_{red2}\cdot10^{-5}$, W/(m^2·K)	0.415	0.480	0.530	0.730	0.990	1.180
	$\alpha_{red(2)}\cdot10^{-5}$,W/(m^2·K)	0.585	0.660	0.728	0.982	1.340	1.620
Two stages	$R_{h.ins}(2)$	0.251	0.211	0.182	0.107	0.056	0.036
	$\alpha_{red}(2)/\alpha_{red1}$	1.200	1.160	1.136	1.073	1.033	1.020
	$R_{h.ins}(2)/R_{h.ins1}$	0.384	0.357	0.319	0.239	0.171	0.137

$$K_1 = 0.411\ \mathrm{Re}_1^{0.646} \quad \text{at} \quad 600 \le \mathrm{Re}_2 \le 6\cdot10^3 \tag{24}$$

for the upper stage, $\varphi = 60^\circ$, $\gamma = 30^\circ$, $\varepsilon = 0.75$, $d_h = 1.6$ mm, $\delta_{ch} = \delta_f = 1.25$ mm, and $h_{ch} = 1.6$ mm.

The lower stage had channels intersecting at an angle $\varphi = 90^\circ$, and its characteristics are given above. For the Re numbers we obtained the following relationship between the stages:

$$\mathrm{Re}\,(2) = 0.885\ \mathrm{Re}\,(1)^{0.943}. \tag{25}$$

Calculation results are given in Table 4. Analyzing the data obtained, we ascertain that use of the second stage is expedient for a substantial reduction in $R_{h.ins}$ since the contribution of the second stage to the reduced heat transfer does not exceed 20–25% even at rather small velocities of the heat-transfer agent ($Re_2 < 600$).

Using the formula for calculating the compactness of a wafer cooling system [5, 6]

$$P = \frac{F_{heat}}{V_{cell}} = \frac{4}{\delta_f} - 2\varepsilon\left(\frac{2}{\delta_f} - \frac{1}{h_{ch}}\right) \tag{26}$$

(where F_{heat} and V_{cell} are the heat-transfer area and the volume of the unit cell of the symmetry of the cooling system), we evaluate the compactness for a size reduction to $\varepsilon = 0.5$–0.75, $\delta_f = 0.3$–1.0 mm, and $h_{ch} = 0.5$–2.0 mm. We obtain $P = 1750$–8700 m^{-1}, which significantly surpasses the range $P = 1000$–1600 m^{-1} investigated above and earlier [5, 6]. Using generalizations of the results [6] and the fact that they are satisfactorily described by formulas obtained in the literature for the heat transfer on the unfinned surface of a "brush" cooling system [11] and for the heat transfer in short channels with a degree of turbulence of the main flow Tu = 10% [12, p. 193], for a hypothetical wafer cooling system with dimensions $\varepsilon = 0.75$, $\delta_f = 0.3$ mm, and $h_{ch} = 0.3$ mm with water cooling (Pr = 7) and a relative velocity Re = 3000 we obtain a reduced heat-transfer coefficient $\alpha_{red} \sim 2.5\cdot10^5$ W/(m^2·K).

The intensification of heat transfer for a multistage cooling system with identical stages will be represented in terms of the corresponding intensification coefficient [8]

$$M_{int}(n) = \frac{\alpha_{red1} - \varepsilon\alpha_f}{\alpha_{red}(1) - \varepsilon\alpha_f} = \frac{\tanh[m_1 h_{\hat{e}} + \varphi_{01} + \varphi_{0n}]}{\tanh\,[m_1 h_{ch} + \varphi_{01}]}, \tag{27}$$

which is the ratio of the contribution of the multistage finning to the heat transfer to the contribution of the finning of just the first stage.

Then the maximum possible $M_{int}(n)$ for this multistage structure with an infinite number of stages ($n \to \infty$) is determined by the formula

$$M_{int\,max} = \tanh\,(m_1 h_{ch} + \varphi_{01})^{-1}\,. \tag{28}$$

The use of several identical stages does not facilitate a strong increase in α_{red}; even when $n \to \infty$ the limiting intensification coefficient calculated by formula (28) for the above structure is $M_{int.max} = 1.2$. At the same time, for one stage $R_{h.ins} = 0.488$, for two stages $R_{h.ins} = 0.238$, and for three stages $R_{h.ins} = 0.116$ (with a thickness of the interchannel baffle $L_b = 0.5$ mm).

Thus, the results obtained in the present work and earlier [4-6] can be employed to determine the hydraulic resistance and heat transfer in wafer structures with different intersection angles of the channels and subsequently, as boundary conditions, in constructing a mathematical model to calculate local flow-rate intensities and temperature fields in two-dimensional regions, using the generalizations obtained with different angles of attack of the structures. The evaluations show that a 3–4-stage wafer cooling system with reduced dimensions permits a practically total heat insulation of the main structure with a rather high reduced heat transfer $\alpha_{red} = (2.5–2.8)\cdot 10^5$ W/(m^2·K).

NOTATION

d_h, hydraulic diameter of the channel, $d_h = 4F_{ch}/\Pi_{ch}$; F_{ch} and Π_{ch}, area and perimeter of the channel; δ_{ch} and h_{ch}, width and height of the channel; φ, intersection angle of the channels; γ, angle of attack (flow); δ_f, thickness of the fin; T, step of the channel in the transverse (S_1) and longitudinal (S_2) directions; ε, porosity, i.e., ratio of the void volume to the total volume of the unit cell of the cooling system; P, compactness, i.e., ratio of the heat-exchange surface area to the volume of the unit cell; $R_{h.ins}$, "heat-insulation" coefficient; G, flow rate; Δp, pressure difference for the distance Δl between the pressure taps; w_{filtr}, filtration rate; $w_1 = w_{filtr}/\varepsilon_m$; $\varepsilon_m = \delta_{ch}/(\delta_f + \delta_{ch})$; $w_2 = w_{filtr}/\varepsilon$; ξ, coefficient of hydraulic resistance; α_{red}, α, α_0, α_v, and α_s, heat-transfer coefficients (reduced, on the fin, on the unfinned portion of the plate, volumetric, surface); q_0, specific heat flux; t_{base}, t_{liq}, t_s, temperature; ϑ, excess temperature in relation to the liquid temperature; ρ and μ_{liq}, density and dynamic viscosity of the liquid; λ and λ_{liq}, thermal conductivities of the material and the liquid; $\mathrm{Re}_i = d_h w_i/\nu_{liq}$, Reynolds number; Pr, Prandtl number; $\mathrm{Nu}_i = \alpha_i d_h/\lambda_{liq}$, Nusselt number; $K_i = \mathrm{Nu}_i \mathrm{Pr}^{-1/3}$, $\eta = \overline{\mathrm{Nu}}/\xi$, and N, criteria of energy efficiency; n, number of stages. Subscripts and superscripts: liq, liquid; s, surface; red, reduced; h.ins, heat insulation; h, hydraulic; ch, channel; f, fin; int, intensification; i = 1–4, number (of the cross section, coefficient, stage velocity, etc.); b, baffle; filtr, filtration; base, base; m, minimum; v, volumetric (coefficient of heat transfer); max, maximum; 0, refers to the heat flux or the number of the coefficient; calc, calculated; exp, experimental.

REFERENCES

1. E. M. Sparrow and V. B. Grannis, *Int. J. Heat Mass Transfer*, **34**, No. 3, 589-600 (1991).
2. V. V. Kharitonov, *Thermophysical Calculation of Laser Mirrors* [in Russian], Moscow (1985).
3. V. V. Kharitonov, *Thermophysics of Laser Mirrors* [in Russian], Moscow (1993).
4. Yu. I. Shanin, V. A. Afanas'ev, O. I. Shanin, and V. N. Fedoseev, *Thermophysics and Nuclear-Power Units* [in Russian], Moscow, 85-89 (1989).
5. Yu. I. Shanin, V. A. Afanas'ev, and O. I. Shanin, *Inzh.-Fiz. Zh.*, **61**, No. 5, 717-725 (1991).
6. Yu. I. Shanin, V. A. Afanas'ev, and O. I. Shanin, *Inzh.-Fiz. Zh.*, **61**, No. 6, 915-924 (1991).
7. V. N. Fedoseev, O. I. Shanin, Yu. I. Shanin, and V. A. Afanas'ev, *Teplofiz. Vys. Temp.*, **27**, No. 6, 1132-1138 (1989).

8. Yu. I. Shanin, V. N. Fedoseev, and O. I. Shanin, *Teplofiz. Vys. Temp.*, **29**, No. 2, 308-316 (1991).
9. V. N. Fedoseev, V. I. Subbotin, and V. V. Kharitonov, *Teploénergetika*, No. 6, 61-64 (1987).
10. E. K. Kalinin, G. A. Dreitser, and S. A. Yarkho, *Intensification of Heat Transfer in Channels* [in Russian], Moscow (1981).
11. V. I. Subbotin, V. V. Kharitonov, A. A. Plakseev, and S. V. Alekseev, *Teploénergetika*, No. 1, 42-44 (1965).
12. A. S. Sukomel, V. I. Velichko, and Yu. G. Abrosimov, *Heat Transfer and Friction in the Turbulent Flow of a Gas in Short Channels* [in Russian], Moscow (1979).